Non-linear dielectric behaviour and glass phase in Sr$_{1-x}$Ca$_x$TiO$_3$ ($x = 0.002$ and $x = 0.003$)

J L Ribeiro†, M T Lacerda-Arôso†, M R Chaves‡, M Maglione§ and A Almeida‡

† Departamento de Física, Escola de Ciências, Universidade do Minho, 4709 Braga, Portugal
‡ Departamento de Física, IMAT (núcleo IFIMUP), CFUP, Faculdade de Ciências da Universidade do Porto, R do Campo Alegre, 687, 4150 Porto, Portugal
§ Laboratoire de Physique du Solide, Université de Bourgogne, P21004 Dijon, France

Abstract. This work reports a study of the temperature and electric field dependence of the dielectric constant of strontium calcium titanate. The first part of the paper is focused on the analysis of a mean-field model for the polar clusters generated by the random impurities of calcium. It is shown that the dipolar moments within each cluster can be represented by an equivalent quantum two-level system. General expressions for the temperature and field dependence of the Edward–Anderson order parameter and of the electrical polarization are given. Analytical solutions are also obtained in the limit of high temperatures and in the limit of high tunnelling frequencies.

The second part of the work reports experimental results on the temperature and electric field dependence of the dielectric constant of strontium calcium titanate (SCT: Sr$_{1-x}$Ca$_x$TiO$_3$), measured along the [100] pseudo-cubic direction, in samples with nominal Ca content of $x = 0.002$ and $x = 0.003$. The analysis of the data suggests that for these low Ca concentrations quantum fluctuations prevent the onset of either a ferroelectric or a glass phase.

1. Introduction

Strontium titanate (ST: SrTiO$_3$) is a well known example of a quantum paraelectric [1]. At room temperature, this material has a cubic perovskite structure (symmetry O$_h$) and, at about $T_{c1} = 105$ K, undergoes a structural antiferrodistorsive phase transition to a tetragonal phase (symmetry D$_{4h}$) [2]. This transition, associated to an anti-symmetric rotation of the oxygen octahedra around the cubic [001] axis, is almost of the second order and is accompanied by an under-damping of the soft mode. At lower temperatures ($T < T_{c1}$), the progressive softening of a long wavelength polar transverse optical mode gives rise to a strong increase of the static dielectric constant [3]. However, the onset of a long range ferroelectric order is suppressed by quantum fluctuations and the rise of the dielectric constant saturates below $T \approx 4$ K [4].

The behaviour of ST at low temperatures appears to be remarkably complex. Measurements of electronic paramagnetic resonance reported by Müller *et al* [5] suggested a possible transition to a quantum regime ($T_{c2} \approx 40$ K), the so-called quantum coherent state (QCS). Subsequent light scattering [6], neutron diffraction [6] and vibrating reed investigations [7] seemed to provide additional evidence for such a phase transition. More recently, it has been shown that the non-linear electric susceptibility displays an anomaly in the vicinity of 35 K, which has been interpreted as due to the transition to the a coherent quantum paraelectric state [8]. However, the nature of this QCS and the characterization of its clear experimental signature remain still unclear in many aspects.

At lower temperatures, ST is extremely sensitive to small amounts of lattice impurities. It is well known that an increase of the concentration of oxygen vacancies ($SrTiO_{3-\delta}$, $\delta > \delta_c$) may stabilize a metallic behaviour and superconductivity [9]. Moreover, the inclusion of non-central ions affects strongly the dielectric properties of the system and may induce ferroelectricity or intermediate ferroelectric glass phases [10].

According to measurements of the linear dielectric constant, strontium calcium titanate (SCT: $Sr_{1-x}Ca_xTiO_3$) seems to reveal ferroelectric ordering for a high enough Ca concentration [11]. As in related systems with non-central impurities, such as $K_{1-x}Li_xTaO_3$ (KTL) or $KTa_{1-x}Nb_xO_3$ (KTN), the inclusion of calcium induces a local dipolar moment very likely related to the Ca^{2+}–V_o (V_o: oxygen vacancy) centres replacing randomly the Ti^{4+}–O^{2-} ion pairs [12–15]. Due to the high polarizability of the host lattice, these dipoles generate a local electric field, polarize locally the lattice and induce random ferroelectric clusters [16]. The polarization within each cluster can be reoriented between several directions dictated by the symmetry of the system. In SCT these directions correspond to the pseudo-cubic directions $[110]_c$ and $\lfloor\bar{1}10\rfloor_c$, perpendicular to the tetragonal $[001]$ axis. Thus, for a high enough Ca concentration, SCT could be an example of a XY, $n = 2$ ferroelectric system with a quartic anisotropy [11].

The stabilization of a long or a short range order in SCT is determined by the competition between the constant sign and the variable sign components of the random fields. In fact, even in a disordered system, local fields of a constant sign may arise from a ferro interaction between the polarized clusters, possibly enhanced by the soft lattice phonons. In incipient ferroelectrics with non-central ions like SCT, a ferroelectric phase and dipolar glass have been observed for $x > x_c$ and $x < x_c$ respectively, x_c being a critical concentration of non-central ions [11].

For low calcium concentrations, the glass phase in SCT may present some similarities with other phases found in disordered systems like spin or orientational glasses. The question whether these systems present or not a thermodynamic transition to a glass phase is still controversial [17, 18]. In fact, while some dynamical properties, like dielectric dispersion, can be described by phenomenological models assuming just a progressive freezing of the dipolar moments of the super-paraelectric clusters near T_f, some static properties seems to agree with mean-field predictions, which state the existence of a true transition to the glass state.

If the freezing temperature T_f corresponds to the thermodynamic transition temperature to the glass phase, then the associated critical behaviour is to be linked to the divergence of the non-linear susceptibility. This prediction is related to the nature of the order parameter involved, which in the paraelectric region may be expressed by the Edwards–Anderson order parameter $q(T, E)$ [19]:

$$q(T, E) = \frac{1}{N} \sum_i [\langle p_i \rangle^2]_{av}.$$

In this equation, N represents the density of polar clusters, p_i the dipolar moment of the ith cluster, and the brackets $\langle\ \rangle$ and [ ] stand respectively for thermal and spatial averages.

The field conjugated to q corresponds to the square of the width of the internal electric field distribution $\langle E \rangle^2$. Thus, the order parameter susceptibility $\partial q/\partial \langle E \rangle^2$ diverges at T_f as the second derivative of the conventional electrical susceptibility. These ideas point out a (in principle) straightforward method for detecting the glass phase transition, by means of the study of the temperature dependence of the non-linear susceptibility in the paraelectric region. Note that by being applied well above T_f this method avoids the difficulties related to the non-ergodic response of the system in the vicinity and below T_f.

The non-linear dielectric constant in SCT has been previously studied by Maglione *et al* [20] and by Kleemann *et al* [16]. In these previous studies, the electric field dependence of the dielectric constant has been fitted to a conventional series expansion in even powers of the electric field, or to this conventional series plus a contribution of two different types of independent polar cluster, calculated by using a Langevin-type approximation. As pointed out in [16], the conventional powers series approach cannot describe accurately the semi-bell shaped $\varepsilon(E)$ curves observed experimentally. On the other hand, the second approach has the drawback of involving at least seven adjustable parameters, which may raise some questions on the interpretation of the data. Moreover, in the two referred models, a strictly classical point of view is adopted, which is clearly at variance with the dominance of the quantum fluctuations in the suppression of the ferroelectric ordering, both in ST and in SCT below the critical concentration [21].

A different point of view has been recently adopted to describe the linear and non-linear dielectric behaviour of pure ST [8]. In order to treat the electric field dependence of the susceptibility and to take into account the effects of quantum fluctuations, these authors consider a transverse Ising Hamiltonian. In a mean-field approximation, this model reproduces the Barrett formula for the linear susceptibility [21] and accounts reasonably well both for the temperature and field dependence of the susceptibility in pure ST.

It is tempting to apply this unified description to the dielectric behaviour of SCT. However, in this case, one must incorporate in the model the effects of disorder due to the random Ca impurities, by considering that the interactions between the clusters have a random component. For the particular case corresponding to a zero tunnelling field ($\Omega = 0$), the problem has been extensively studied and, in a mean-field approximation, leads to the Sherrington–Kirkpatrick model [22] (S–K), which is known to be well adapted to the description of spin glasses.

In the first part of this paper we adopt the guidelines of the S–K model and, by considering a non-zero tunnelling amplitude, deduce the general expressions for the electrical polarization and for the Edwards–Anderson order parameter as functions of the temperature and field. Then, in order to obtain analytical expressions for the electrical susceptibility, we consider the solutions corresponding to high temperature limit and to the high tunnelling amplitude limit. In the second part, we apply this latter approximation to the analysis of the linear and non-linear dielectric constants of SCT. It is shown that the experimental data obtained in samples with low Ca concentrations ($x = 0.2$ at.% and $x = 0.3$ at.%) can be consistently described by the model. This analysis allows a calculation of the relevant parameters of each Ca concentration, namely the number of clusters per unit of volume, the average dipole moment per cluster, the Curie temperature T_0, the freezing temperature T_f and the tunnelling temperature T_1. The results show that, for this low Ca concentrations, the quantum fluctuations stabilize the paraelectric phase and prevent the onset of either a ferro- or a glass stable phase. Finally, in the third part, some conclusions are drawn from this analysis and some speculations are made on the possible onset of a ferro- or a glassy phase at higher Ca contents.

2. Theory

As referred to above, the easy axes of the polarization in SCT are the cubic [110] and $\lfloor 1\bar{1}0 \rfloor$ directions in the (001) plane. For an electric field applied along [100], these two directions are energetically equivalent. We can therefore describe the polar states by effective up $|+\rangle$ or down $|-\rangle$ states, depending on whether their [100] component of the polarization is parallel or anti-parallel to the applied electric field.

Due to the high polarizability of the lattice, the local dipolar fields generated by the non-central Ca ions are expected to break locally the tetragonal (D_{4h}) symmetry of the paraelectric

lattice and to induce local highly correlated ferro domains with a C_{2v} orthorhombic symmetry. Hence, for low calcium concentrations and for high enough temperatures, these polar clusters are expected to interact very weakly with each other. The system thus behaves nearly like a quantum 'superparaelectric'.

In order to describe the dielectric response of the system, we firstly associate with each polar cluster an effective quantum two-level system characterized by a certain Ising dipolar moment η and a certain tunnelling energy A. In the presence of a local electric field E, the Hamiltonian of a single cluster is then:

$$h = \begin{bmatrix} \eta E & -A \\ -A & -\eta E \end{bmatrix}. \tag{1}$$

This Hamiltonian has the following eigenvectors and eigenvalues:

$$|\psi_+(z)\rangle = \cos\left(\frac{\theta(z)}{2}\right)|+\rangle - \sin\left(\frac{\theta(z)}{2}\right)|-\rangle \qquad e_+ = +\sqrt{A^2 + \eta^2 E^2(z)} \tag{2a}$$

$$|\psi_-(z)\rangle = \sin\left(\frac{\theta(z)}{2}\right)|+\rangle + \cos\left(\frac{\theta(z)}{2}\right)|-\rangle \qquad e_- = -\sqrt{A^2 + \eta^2 E^2(z)} \tag{2b}$$

with

$$\theta(z) = \tan^{-1}\left(-\frac{A}{\eta E(z)}\right).$$

The dipolar moment of each eigenstate is:

$$\langle\Psi_+|D|\Psi_+\rangle = -\langle\Psi_-|D|\Psi_-\rangle = \eta\frac{\eta E}{\sqrt{A^2 + \eta^2 E^2}} = \eta\cos(\theta). \tag{3}$$

Note that a finite tunnelling integral A effectively reduces the magnitude of the dipolar moment of the cluster.

The next step is to consider the interaction between random distributed clusters. One must then consider a complete Hamiltonian that includes the coupling between the dipolar moments of the different clusters:

$$H = \sum_i h_i + \frac{1}{2}\sum_i\sum_j J_{ij}\eta_i\eta_j. \tag{4}$$

In this equation, h_i represents the single-cluster Hamiltonian given by equation (1).

We adopt, in addition, a mean-field approximation, which is known to be quite satisfactory above the Almeida–Thouless line [23], for systems with long range interactions. It seems therefore reasonable to apply this approach to a system like SCT, where dipolar long range interactions play an important part.

By adopting these guidelines we are led to the grounds of the Sherrington–Kirkpatrick model for spin glasses. Note that, in this approximation, the coupling between dipoles affects the value of the local electric field. As in the S–K model, one assumes that the distribution of dipolar interactions is a Gaussian characterized by a certain average value J_0 and a certain width J_1, which can be associated respectively with the constant sign and random sign components of a local electrical field $E(z)$, which is a function of a random variable z [22]:

$$E(z) = E + J_0 P + J_1 q^{1/2} z. \tag{5}$$

In this equation, P is the electrical polarization and q the Edward–Anderson order parameter. These quantities can be expressed as:

$$P = \frac{N\eta}{\sqrt{2\pi}}\int_{-\infty}^{+\infty} e^{-(z^2/2)}\frac{\eta E(z)}{\sqrt{A^2 + \eta^2 E^2(z)}}\tanh\left[\frac{\sqrt{A^2 + \eta^2 E^2(z)}}{k_B T}\right]dz \tag{6}$$

$$q = \frac{\eta^2}{\sqrt{2\pi}}\int_{-\infty}^{+\infty} e^{-(z^2/2)}\frac{\eta^2 E^2(z)}{A^2 + \eta^2 E^2(z)}\tanh^2\left[\frac{\sqrt{A^2 + \eta^2 E^2(z)}}{k_B T}\right]dz. \tag{7}$$

Note that the set of equations (5)–(7) is similar but not equivalent to the one obtained previously for proton glasses like RADP, where a random-bond transverse Ising model in a longitudinal random field is adopted [24, 25].

Equations (5)–(7) must be solved numerically. However, it is possible to obtain analytical solutions in the limits of high temperatures or high tunnelling frequencies.

2.1. High temperature limit ($k_B \gg \sqrt{A^2 + \eta^2 E^2(z)}$)

In this case one can take, as a first approximation:

$$\tanh^2\left[\frac{\sqrt{A^2 + \eta^2 E^2(z)}}{k_B T}\right] \approx \left[\frac{A^2 + \eta^2 E^2(z)}{(k_B T)^2}\right] + \cdots. \tag{8}$$

By replacing (5) and (8) into (7) we can estimate the temperature and field dependence of the order parameter $q(T, E)$ in the paraelectric phase:

$$q(T, E) \approx \frac{\eta^4 (E + J_0 P)^2}{k_B(T^2 - T_f^2)} \tag{9}$$

where $T_f = \eta^2 J_1 / k_B$ represents the freezing temperature of the cluster gas.

By replacing (9) into (5) and (6) and taking into account the expansion $\tanh(x) \approx x - \frac{1}{3}x^3 + \frac{2}{15}x^5 + \cdots$, we can obtain the following polynomial expansion for the electric polarization:

$$P(T, E) = \frac{\varepsilon C_1 E}{(T_1/2)\coth(T_1/2T) - T_0}$$
$$- \frac{\varepsilon C_3 E^3}{3T^3}\left[\frac{(T_1/2)\coth(T_1/2T)}{(T_1/2)\coth(T_1/2T) - T_0}\right]^4 \frac{T^2 + 2T_f^2}{T^2 - T_f^2} + \cdots \tag{10}$$

where

$$C_1 = \frac{N\eta^2}{k_B \varepsilon_0} \qquad C_3 = \frac{N\eta^4}{k_B^3 \varepsilon_0} \qquad T_0 = \frac{N\eta^2 J_0}{k_B} \quad \text{and} \quad T_1 = \frac{2A}{k_B}.$$

At high temperatures, the linear susceptibility follows the Barrett formula and its temperature dependence is not affected by the random disorder ($J_1 \neq 0$). However, the non-linear susceptibility exhibits a non-analytic behaviour at $T = T_f$. Note that, in the classical limit ($T_1 \to 0$), one obtains the Sherrington–Kirkpatrick results for high temperatures: $\chi_1(T, E)$ follows a Curie–Weiss law and

$$\chi_3(T, E) = CT\left[\frac{1}{T - T_0}\right]^4 \frac{T^2 + 2T_f^2}{T^2 - T_f^2}.$$

2.2. High tunnelling frequencies ($\eta E(z)/A \ll 1$)

If the tunnelling energy $A = k_B T_1$ dominates over the local Zeeman energy (i.e. if $T_1 > 2T_0$, $T_1 > 2T_f$ and the applied electric fields are small), it is possible to expand the hyperbolic tangent as:

$$\tanh\left[\frac{\sqrt{A^2 + \eta^2 E^2(z)}}{k_B T}\right] = \tanh\left[\frac{A}{k_B T}\left(1 + \frac{\eta^2 E^2(z)}{A^2}\right)^{1/2}\right]$$
$$\approx \tanh\left[\frac{T_1}{2T}\left(1 + \frac{2\eta^2 E^2(z)}{k_B^2 T_1^2} + \cdots\right)\right]$$
$$\approx \tanh\left[\frac{T_1}{2T}\right] + \frac{\eta^2 E^2(z)}{k_B T_1 T}\operatorname{sech}^2\left[\frac{T_1}{2T}\right] + \cdots \tag{11}$$

and the other integrand functions as:

$$\frac{1}{\sqrt{A^2 + \eta^2 E^2(z)}} \approx \frac{2}{k_B T_1} \left(1 - \frac{2\eta^2 E^2(z)}{k_B^2 T_1^2} + \cdots\right) \tag{12a}$$

$$\frac{1}{A^2 + \eta^2 E^2(z)} \approx \left(\frac{2}{k_B T_1}\right)^2 \left(1 - \frac{4\eta^2 E^2(z)}{k_B^2 T_1^2} + \cdots\right). \tag{12b}$$

It is then easy to show that, in this approximation and up to terms in E^2, the Edwards–Anderson order parameter $q(T, E)$ and the electric polarization $P(T, E)$ can be written respectively as:

$$q(T, E) \approx \frac{(4\eta^4/k_B T_1^2) \tanh^2(T_1/2T)[E + (T_0/\varepsilon_0 C_1) P(T, E)]^2}{1 - 4(T_f/T_1)^2 \tanh^2(T_1/2T)} \tag{13a}$$

and

$$\begin{aligned}
P(T, E) &\approx \mathcal{E}^{(1)} E - \mathcal{E}^{(3)} E^3 + \cdots = \frac{\varepsilon_0 C_1}{(T_1/2) \coth(T_1/2T) - T_0} E \\
&\quad - \varepsilon_0 D_3 \left[\frac{4 \tanh(T_1/2T) - 2(T_1/T) \operatorname{sech}^2(T_1/2T)}{(1 - 2(T_0/T_1) \tanh(T_1/2T))^4}\right] \\
&\quad \times \left[\frac{T_1^2 + 8T_f^2 \tanh^2(T_1/2T)}{T_1^2 - 4T_f^2 \tanh^2(T_1/2T)}\right] E^3 + \cdots
\end{aligned} \tag{13b}$$

where

$$D_3 = \frac{N\eta^4}{\varepsilon_0 k_B^3 T_1^3}.$$

The dominance of the quantum fluctuations prevents not only the divergence of the linear susceptibility (according to the Barrett formula if $T_1 > 2T_0$) but also suppress the divergence of the non-linear susceptibility as $T \to T_f$ if $T_1 > 2T_f$. Thus, in the limit considered, both the ferro and the glass phases are destabilized by the quantum fluctuations.

The model discussed incorporates the basic ingredients to describe the competitions between the ferroelectric, the paraelectric and the cluster glass phases that may occur in disordered systems like SCT. In order to generate a phase sequence for an arbitrary set of parameters T_0, T_1 and T_f, the model must be solved numerically.

The analysis of the dielectric behaviour of ST shows that the quantum fluctuations are clearly dominant and stabilize the paraelectric phase. One can therefore expect that in low Ca doped SCT the high tunnelling frequency limit discussed above can be applied. In the next part we will discuss the experimental results obtained in low doped Ca SCT by using equations (13a) and (13b).

3. Results and discussion

The dielectric constant was measured as a function of temperature and electric field with an HP 4192A *LCR*-meter. The SCT samples, cut as parallel plates perpendicular to the [100] cubic direction, had typical dimensions of $2.5 \times 2.5 \times 0.25$ mm^3 and the major faces were electroded by gold vapour deposition. The electric field dependence of the dielectric constant was measured with a four-probe method and at constant temperature, the temperature stability being better than 0.1 K. In the measurements, the amplitude of the static electric field was always smaller than 200 V cm^{-1} because higher fields are expected to induce a ferroelectric phase, even in the pure compound [8]. The data were registered for increasing and decreasing electric fields. In the temperature range considered no hysteresis was found. The temperature

(a)

(b)
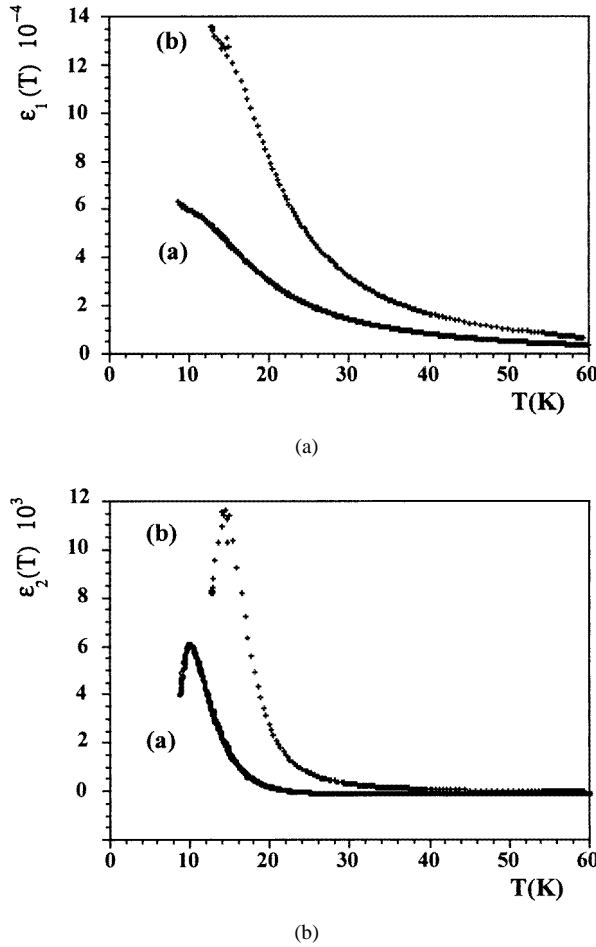
Figure 1. (a) Temperature dependence of the real part of the linear dielectric constant measured for $x = 0.002$ (curve (a)) and for $x = 0.003$ (curve (b)). (b) Temperature dependence of the imaginary part of the linear dielectric constant measured for $x = 0.002$ (curve (a)) and for $x = 0.003$ (curve (b)).

rate was always smaller than 0.3 K min^{-1}. No special care was taken to obtain a monodomain crystal in the tetragonal phase ($T < T_c \approx 105$ K).

Figure 1 shows the temperature dependence of the real $\varepsilon(T)$ and imaginary $\varepsilon_2(T)$ parts of the linear dielectric constant measured in the $x = 0.002$ (curves (a)) and $x = 0.003$ (curves (b)) samples, at a frequency of 10 kHz. As in pure ST we observe that, in both samples and for this frequency, $\varepsilon(T)$ rises monotonically as the temperature decreases down to 9 K. The magnitude of the dielectric constant strongly increases with the Ca content. The imaginary part displays a clear maximum at about $T_m = 10$ K for $x = 0.002$ and at $T_m = 15$ K for $x = 0.003$. Similar dielectric loss peaks near 10 K are also observed in pure ST [8] as well as in other similar perovskites like KTa$_{1-x}$Nb$_x$O$_3$ [26]. The origin of these anomalies has been ascribed either to solitonic excitations between mutually tilted domains [8] or to polaronic excitations [26]. Note that in the special case of ST the polaronic excitations occur within the 'coherent quantum phase' and are sensitive to quantum fluctuations. Accordingly, the concept
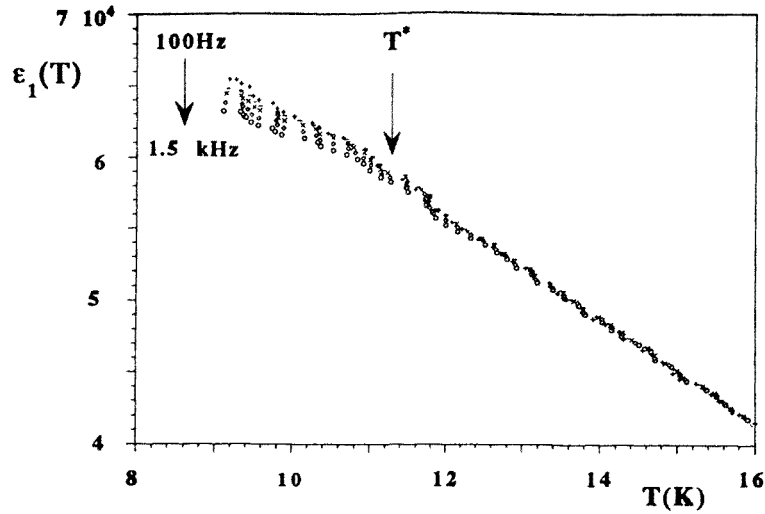
(a)
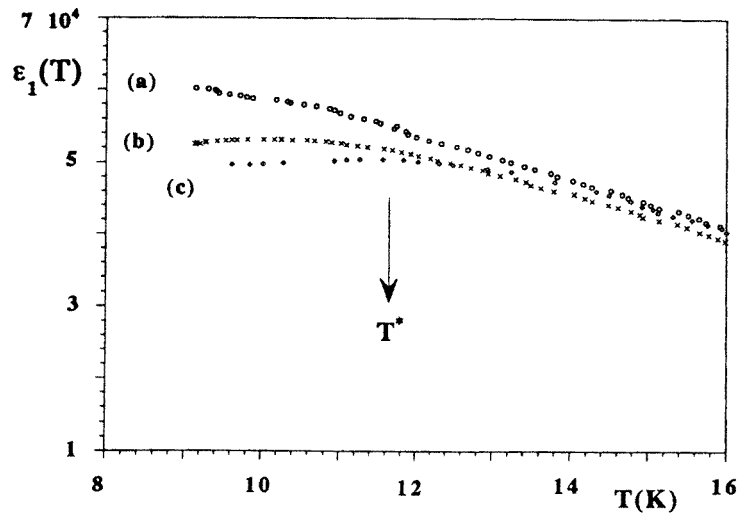
(b)

Figure 2. (a) The dielectric constant $\varepsilon_1(T)$ measured in an $x = 0.002$ sample, using a constant ac field (20 V cm^{-1}) and different frequencies, in the range 100 Hz–1.5 kHz. (b) The dielectric constant $\varepsilon_1(T)$ measured in an $x = 0.002$ sample, using a constant frequency (10 kHz) and different ac fields (a—20 V cm^{-1}, b—4 V cm^{-1} and c—2 V cm^{-1}).

of a quantum polaron has been introduced and related to the loss anomalies observed in SC and SCT at low temperatures [27].

As the temperature decreases towards T_m one observes that the dielectric response at zero bias field becomes dependent on the measuring parameters adopted. This observation is illustrated in figure 2 for the $x = 0.002$ samples. Figure 2(a) displays $\varepsilon_1(T)$ measured with an ac field of 20 V cm^{-1} and different frequencies ranging from 100 Hz to 1.5 kHz. As can be seen, a clear frequency dispersion is observed below a temperature $T^* > T_m$. Figure 2(b) shows $\varepsilon_1(T)$ measured in the same sample at a constant frequency of 10 kHz but with different ac fields

(20 V cm^{-1} (a), 4 V cm^{-1} (b) and 2 V cm^{-1} (c)), showing that the dielectric response becomes dependent on the amplitude of the measuring field. At low measuring fields (e.g. 2 V cm^{-1}) a maximum in $\varepsilon_1(T)$ is observed. The temperature corresponding to this maximum depends both on the amplitude and frequency of the measuring field.

In order to estimate the mean-field parameters that characterize the dielectric response of the samples we must focus on a temperature range where its dependence on the measuring parameters can be neglected. For the frequencies and ac fields scanned (100 Hz–100 kHz, 2–20 V cm^{-1}) this region corresponds to temperatures above $T^* \approx 11$ K ($x = 0.002$) and $T^* \approx 16$ K ($x = 0.003$).
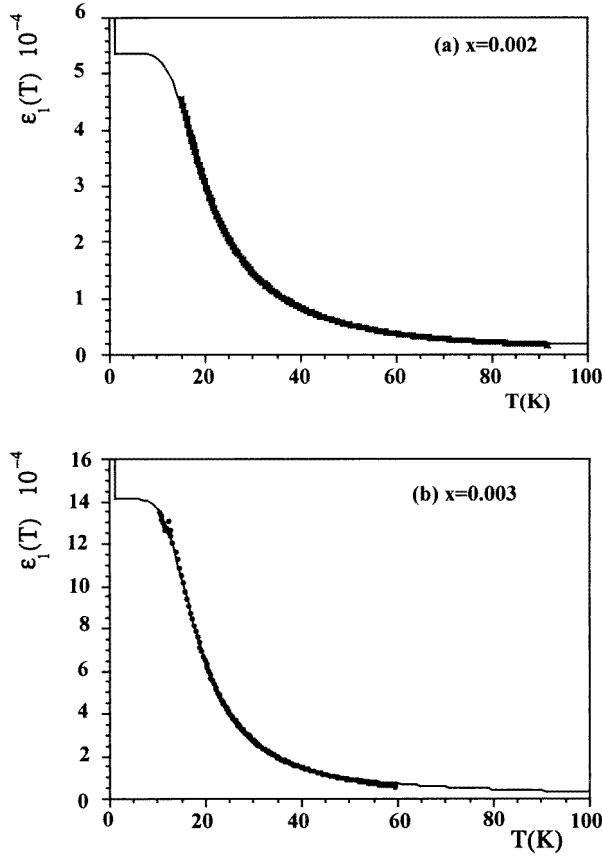
Figure 3. (a) Fit of $\varepsilon_1(T)$ measured for $x = 0.002$ (10 kHz and 20 V cm^{-1}) to the Barrett formula ($C_1 = 139\,500$ K; $T_1 = 68$ K; $T_0 = 32$ K). (b) Fit of $\varepsilon_1(T)$ measured for $x = 0.003$ (10 kHz and 20 V cm^{-1}) to the Barrett formula ($C_1 = 234\,950$ K; $T_1 = 72$ K; $T_0 = 34$ K).

Figures 3 show the temperature dependence of $\varepsilon_1(T)$ in the temperature range above T^* for the two compositions in analysis. In the same figures the fit of the data to the Barrett formula is shown. As can be seen, and in agreement with previous results [28], the temperature dependence of $\varepsilon_1(T)$ can be well described by the Barrett equation:

$$\varepsilon_1(T) \approx \frac{C_1}{(T_1/2)\coth(T_1/2T) - T_0}.$$

The parameters fitted to the experimental curves are $C_1 = 139\,500$ K, $T_0 = 32$ K and $T_1 = 68$ K

for $x = 0.002$ and $C_1 = 234\,950$ K, $T_0 = 34$ K and $T_1 = 72$ K for $x = 0.003$. As in these compositions $T_1 > 2T_0$, the linear dielectric constant does not diverge at a finite temperature and tends to saturate as the temperature decreases: the quantum fluctuations suppress the ferroelectric order. Moreover the high values fitted to T_1 show that, in both samples, the quantum fluctuations are dominant over the cluster interactions and over the thermal energy in a temperature region where dielectric non-linearities are observed. This fact suggests that the high tunnelling energy limit, described in the previous section, may be used in order to describe also, in a simple way, the electric field dependence of the dielectric response (see equation (13b).

Let us first note that, as previously reported [16], the experimental $\varepsilon(E)$ curves display a semi-bell-shape that cannot be accurately described by using a conventional ε versus E polynomial expansion involving merely even powers of the electric field. This means that the high tunnelling frequency limit, giving rise to such a polynomial $\varepsilon(E)$ expansion, is not expected to describe this field dependence for arbitrarily high fields. In fact, this is not surprising as the high frequency tunnelling limit itself fails for high fields (as T_0 and T_f are increased by the applied field). One can however apply such a limit if the analysis is restricted to the low field region of the $\varepsilon(E)$ curves for which higher order non-linearities can be neglected and $\varepsilon(E)$ varies linearly with E^2.

Figure 4 displays the isothermal dependence of $\varepsilon(T)$ on the square of the applied dc field E^2. According to the ideas referred above, the lower order non-linear dielectric constant $\varepsilon_1^{(3)}(T)$ can be estimated by calculating the slope of the experimental curves $\varepsilon_1(E^2)$ at the limit $E \to 0$. The non-linear dielectric constant obtained by this method is shown in figure 5(a) as a function of temperature. Note that this temperature dependence can be fitted to the one predicted in equation (13b), by using only two adjustable parameters T_f and D_3. The values of the two parameters fitted to the two compositions are $D_3 = 2 \times 10^{-10}$ m^2 V^{-2} and $T_f = 29.5$ K ($x = 0.002$) and $D_3 = 1.3 \times 10^{-10}$ m^2 V^{-2} and $T_f = 36$ K ($x = 0.003$). The extrapolation of the fitted curves towards lower temperatures (figures 5(b) and (c)) suggests that the non-linear dielectric constants saturate, in both samples, as the temperature decreases. This saturation seems to indicate that an eventual glass phase is effectively suppressed by the quantum fluctuations.

Table 1.

	C_1 [K]	D_3 [m^2 V^{-2}]	T_1 [K]	T_0 [K]	T_f [K]	N [m^{-3}]	η [eA]
$x = 0.002$	139 500	1.0×10^{-8}	68	32	29	1.8×10^{26}	19
$x = 0.003$	234 950	1.4×10^{-8}	72	34	36	4.1×10^{26}	17

Table 1 summarizes the values of the parameters C_1, D_3, T_0, T_1 and T_f fitted to $\varepsilon_1(T)$ and $\varepsilon_1^{(3)}$. From these parameters we can estimate the density of clusters N (m^{-3}) and the average dipolar moment per cluster η (eA) (see table 1). In nominally pure ST, Hemberger *et al* [8] found $N = 3.6 \times 10^{26}$ m^{-3} and $\eta = 12$ eA. Note that the values for the pure compound result from measurements of $\varepsilon_1(T, E)$ at a frequency of 85 kHz and over a wide range of temperatures (5–100 K), as well as from the assumption of $T_f = 0$ implicit in the model adopted by the authors.

As pure ST has a density of Ti^{4+} ions of the order of $N_0 = 1.6 \times 10^{28}$ m^{-3}, we can also estimate the average size of a cluster. This value is of about 40 unit cells in $x = 0.003$ and of about 90 unit cells in $x = 0.002$, values that correspond to the volume of a sphere with a radius of the order of 1 nm. At the same time, the average dipolar moment per unit cell keeps a value of the order of 0.2–0.3 eA.

In conclusion, the results described above indicate that, for the low amounts of Ca con-
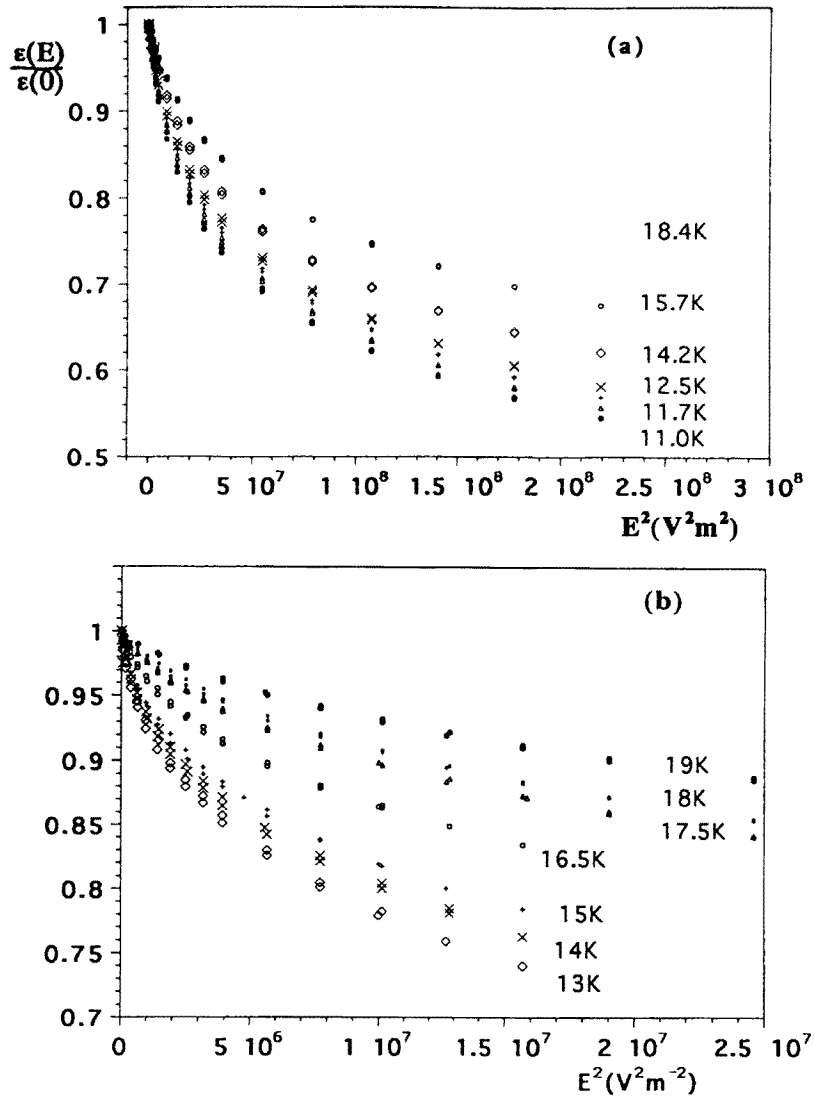
Figure 4. Isothermal $\varepsilon_1(E^2)$ curves measured at different temperatures for $x = 0.002$ (figure 4(a)) and for $x = 0.003$ (figure 4(b)).

sidered, the system of the polar nano-clusters may be described as a quantum paraelectric, as $T_1 > 2T_0$ and $T_1 > 2T_f$. However, the rapid increase of T_f suggests that for higher concentrations of Ca random sign interaction between cluster may dominate and a glass phase may be stabilized. In fact, the critical composition x_c above which a glass phase may be stabilized seems very close to $x \approx 0.003$, as the values fitted to this composition indicate that $T_1 \approx 2T_f$.

4. Final remarks

The description of the polar clusters generated by the Ca impurities in SCT as a weakly interacting quantum two-level system allows a simple analysis of the temperature and electric
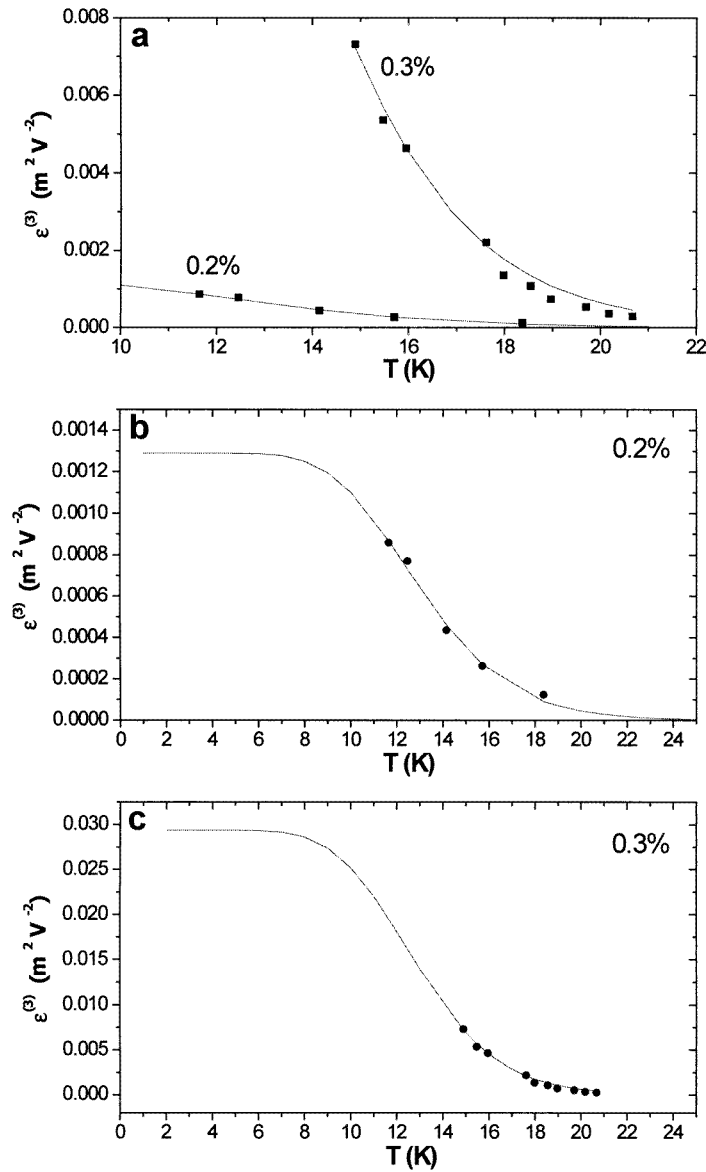
Figure 5. (a) First order non-linear dielectric constants deduced from the experimental curves $\varepsilon_1(E^2)$ for $x = 0.002$ and $x = 0.003$. The lines shown correspond to the fits of the data to the non-linear term in equation (13). (b) Extrapolation towards lower temperatures of curve adjusted to the non-linear dielectric constant for $x = 0.002$. (c) Extrapolation towards lower temperatures of curve adjusted to the non-linear dielectric constant for $x = 0.003$.

field dependence of the dielectric constant measured in samples with low Ca concentrations. In the two compositions studied, the analysis of the experimental data suggests that quantum fluctuations stabilize the paraelectric phase and prevent a divergence of the linear and non-linear dielectric constants. The temperature T_f increases strongly with the Ca content and may give rise to a divergence of the non-linear susceptibility at a higher Ca concentration. Of course, the application of the model to $x > x_c$ would require a numerical fit of equations (7)

and (8) to the experimental data, rather than the use of the simplified equation (13). This work is being carried out presently and may confirm the existence of a glass phase in SCT for intermediate Ca contents.

Acknowledgments

References

[1] Müller K A and Burkard H 1979 *Phys. Rev.* B **19** 3593
[2] Shirane G and Yamada Y 1969 *Phys. Rev.* **177** 858
[3] Cowley R A 1962 *Phys. Rev. Lett.* **9** 159
[4] Viana R, Lunkenheimer P, Hemberger J, Böhmer R and Loidl A 1994 *Phys. Rev.* B **50** 601
[5] Müller K A, Berlinger W and Tosatti E 1991 *Z. Phys.* B **48** 277
[6] Vacher R, Pelous J, Hennion B, Goddens G, Courtens E and Müller K A 1992 *Europhys. Lett.* **17** 45
[7] Nes O M, Müller K A, Suzuki P and Fossheim F 1992 *Europhys. Lett.* **19** 397
[8] Hemberger J, Nicklas M, Viana R, Lunkenheimer P, Loidl A and Böhmer R 1996 *J. Phys.: Condens. Matter.* **8** 4673
[9] Gervais F, Servoin J L, Baratoff A, Bednorz J G and Binnig G 1993 *Phys. Rev.* B **47** 8187
[10] Vugmeister V E and Glinchuk M D 1990 *Rev. Mod. Phys.* **62** 993
[11] Bednorz J G and Müller K A 1984 *Phys. Rev. Lett.* **52** 2289
[12] Höchli U, Weibel H E and Boatner L A 1978 *Phys. Rev. Lett.* **41** 1410
     Höchli U, Weibel H E and Boatner L A 1979 *J. Phys. C: Solid State Phys.* **12** L563
[13] Höchli U, Kofel P and Maglione M 1985 *Phys. Rev.* B **32** 4546
[14] Yacoby Y 1981 *Z. Phys.* B **41** 269
[15] Prater R L, Chase L C and Boatner L A 1981 P *Phys. Rev.* B **23** 5904
[16] Bianchi U, Dec J, Kleemann W and Bednorz J G 1995 *Phys. Rev.* B **51** 8737
[17] Binder K and Young A P 1986 *Rev. Mod. Phys.* **58** 801
[18] Pappa C and Hanrman J 1985 *J. Physique* **46** 637
[19] Edwards S F and Anderson P W 1975 *J. Physique* **5** 965
[20] Maglione M, Lopes dos Santos M, Chaves M R and Almeida A 1994 *Phys. Status Solidi* b **181** 73
[21] Barrett J H 1952 *Phys. Rev.* **86** 118
[22] Sherrington D and Kirkpatrick S 1979 *Phys. Rev. Lett.* **23** 1754
[23] Almeida J L R and Thouless D J 1978 *J. Phys. A: Math. Gen.* **11** 983
[24] Pirc R, Tadic B and Blinc R 1985 *Z. Phys.* B **61** 69
     Pirc R, Tadic B and Blinc R 1987 *Phys. Rev.* B **36** 8607
[25] Pirc R, Tadic B and Blinc R 1994 *Physica* B **196** 109
[26] Bidault O, Maglione M, Actis M, Kchikech M and Salce B 1995 *Phys. Rev.* B **52** 4191
[27] Maglione M 1996 *Ferroelectrics* **176** 1
[28] Chaves M R, Almeida A, Maglione M and Ribeiro J L 1996 *Phys. Status Solidi* b **197** 232